

Supporting Information for

**Molecular Modeling of Shockwave-mediated Delivery
of Paclitaxel Aggregates across the Neuronal Plasma
Membrane**

Mi Zhou,^{a,b} Wenyu Zhou,^a Hong Yang,^a Luoxia Cao,^a Ming Li,^a and Yang Zhou^{a,}*

^a Institute of Chemical Materials, Chinese Academy of Engineering and Physics,
621900 Mianyang, China;

^b School of Materials Science & Engineering, Beijing Institute of Technology, 100081
Beijing, China.

AUTHOR INFORMATION

Corresponding Author

*Yang Zhou. E-mail: zhouy@caep.cn

Captions

Table S1. The composition of plasma membrane.

Figure S1. All systems used in this simulation.

Figure S2. Pressure versus time curve at membrane surface when $D = 10$ (a), 20 (b), 30 (c), 40 (d) and 50 nm, respectively, $u_p = 0.9$ km/s.

Figure S3. The radius of gyration (Rg) of PTX cluster during shock process when $D = 10, 20, 30, 40,$ and 50 nm, respectively.

Figure S4. Pore area vs shock simulation time under bubble arrangement with slanted (Model 6 and 7), parallel (Model 8), serial (Model 9) and single bubble (Model 2), all bubble diameter is 20 nm. The shock wave can rebound in 100 ps simulation time, so we only analyze the non-rebound stage, the solid line.

Figure S5. Delayed snapshot of the dynamic process of recovery simulation when the penetration depth of PTX is (a) 11.6 nm (after 78 ps shock wave when $D = 20$ nm, $u_p = 1.1$ km/s); (b) 18.7 nm (after 100 ps shock wave when $D = 40$ nm, $u_p = 0.7$ km/s); (c) 20 nm (after 40 ps shock wave when $D = 40$ nm, $u_p = 1.1$ km/s); (d) 37.7 nm (after 70 ps shock wave when $D = 40$ nm, $u_p = 1.1$ km/s) and (e) 21.2 nm (after 86 ps shock wave when $D = 30$ nm, $u_p = 0.9$ km/s), respectively.

Table S1. The composition of plasma membrane.

Composition name	Number of lipids		Total
	Outer leaflet	Inner leaflet	
Phosphatidylcholine (PC)	2412	1288	3700
Phosphatidylethanolamine (PE)	1093	2017	3110
Sphingomyelin (SM)	892	219	1111
Phosphatidylserine (PS)	0	930	930
Glycolipid (GM1)	135	0	135
Glycolipid (GM3)	135	0	135
Cerebrosides (CERE)	742	0	742
Phosphatidylinositol (PI)	0	484	484
Phosphatidic acid (PA)	0	38	38
Phosphatidylinositol phosphates (PIPs)	0	132	132
Ceramide (CER)	56	55	111
Lysophosphatidylcholine (LPC)	30	15	45
Lysophosphatidylethanolamine (LPE)	15	30	45
Diacylglycerol (DAG)	38	38	76
Cholesterol (CHOL)	4431	4222	8653
Total lipids	9979	9468	19435

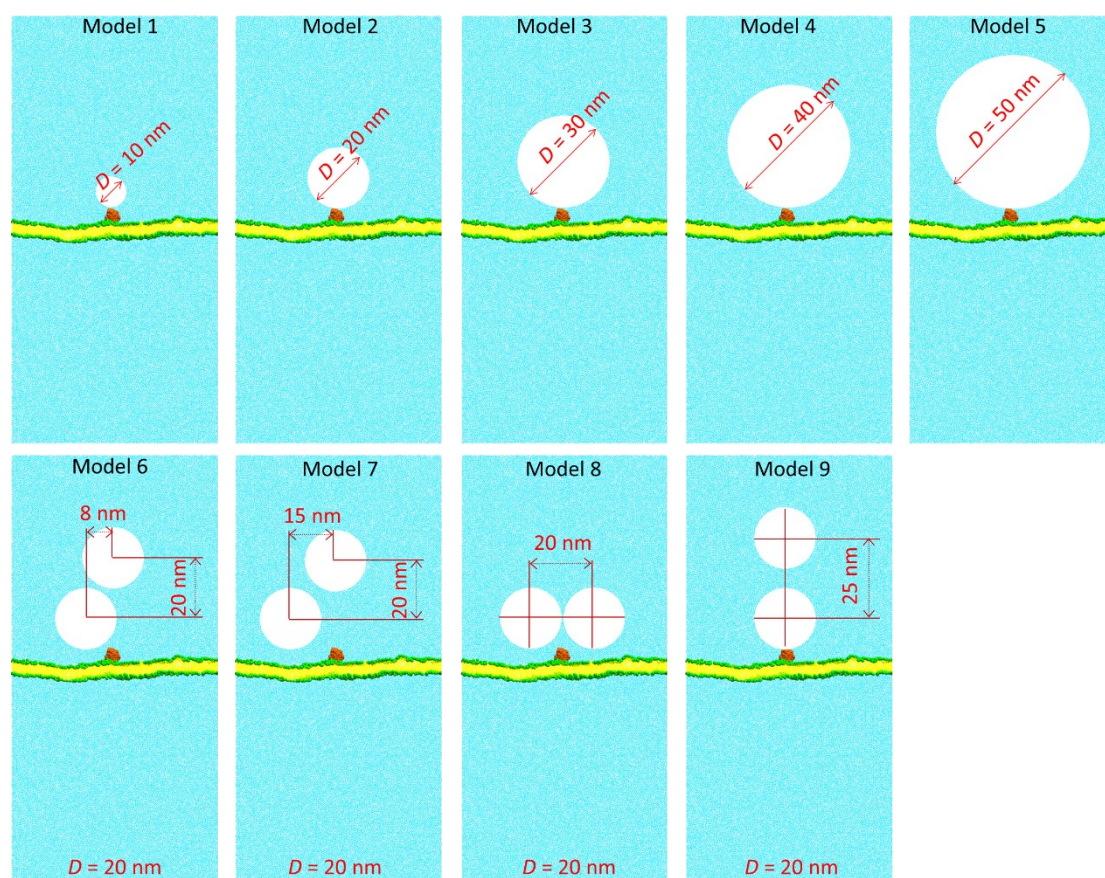


Figure S1. All systems used in this simulation.

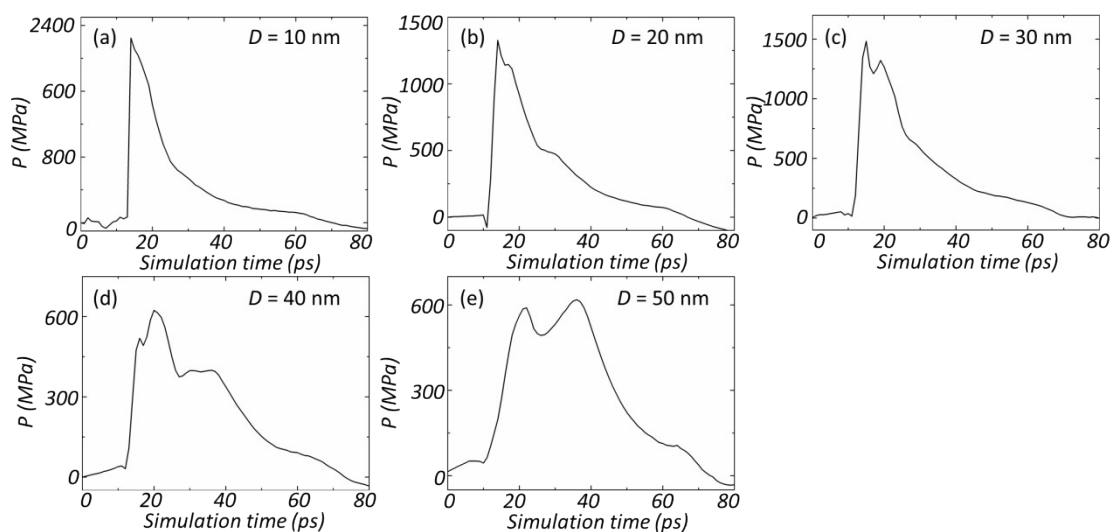


Figure S2. Pressure versus time curve at membrane surface when $D = 10$ (a), 20 (b), 30 (c), 40 (d) and 50 nm, respectively, $u_p = 0.9$ km/s.

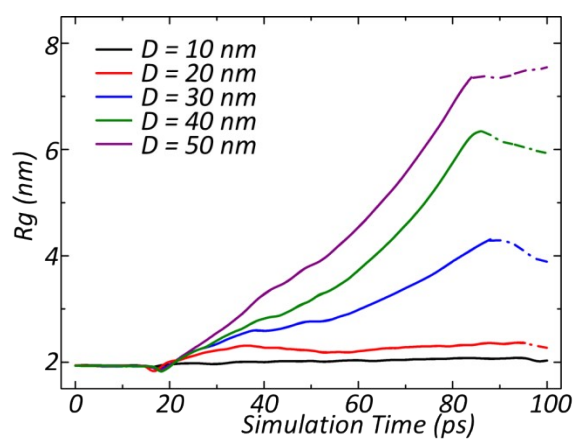


Figure S3. The radius of gyration (R_g) of PTX cluster during shock process when $D = 10, 20, 30, 40,$ and 50 nm, respectively.

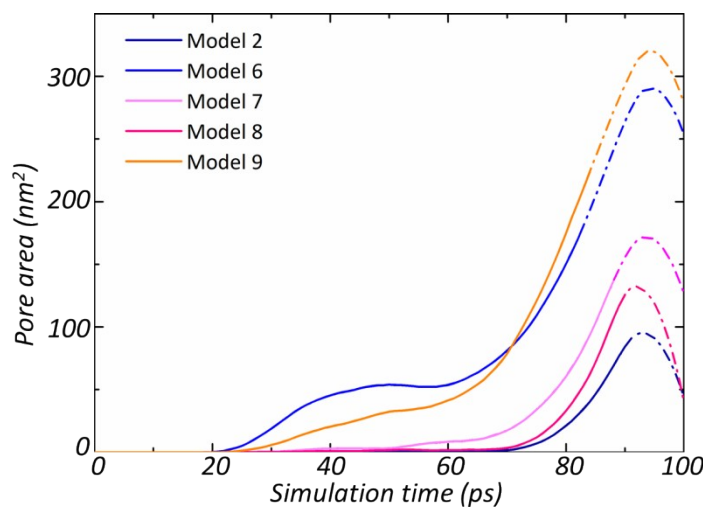


Figure S4. Pore area vs shock simulation time under bubble arrangement with slanted (Model 6

and 7), parallel (Model 8), serial (Model 9) and single bubble (Model 2), all bubble diameter is 20 nm, $u_p = 0.9$ km/s. The shock wave can rebound in 100 ps simulation time, so we only analyze the non-rebound stage, the solid line.

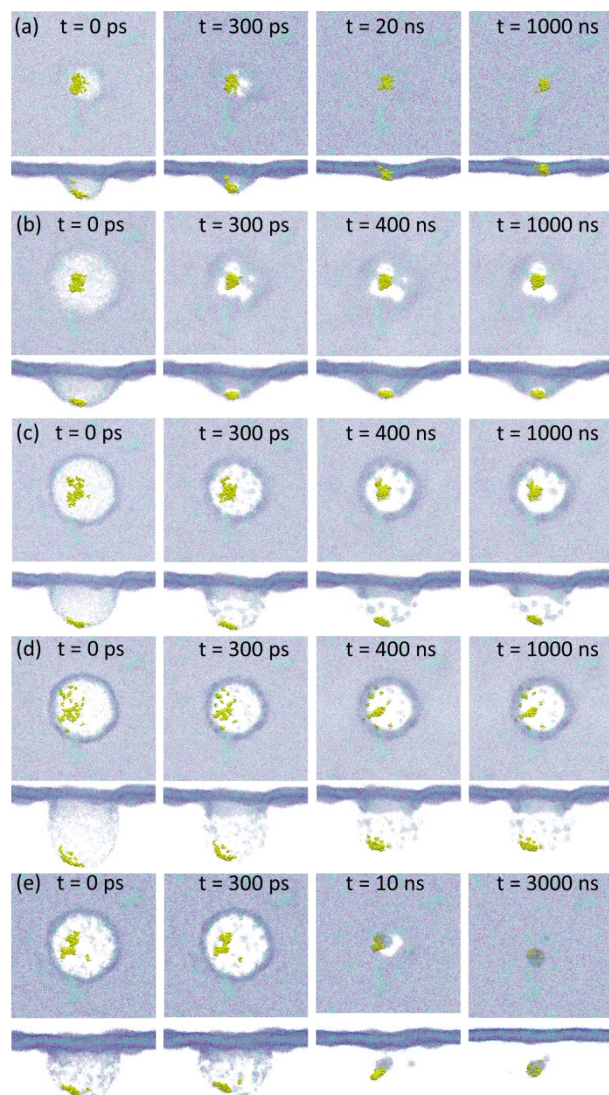


Figure S5. Delayed snapshot of the dynamic process of recovery simulation when the penetration depth of PTX is (a) 11.6 nm (after 78 ps shock wave when $D = 20$ nm, $u_p = 1.1$ km/s); (b) 18.7 nm (after 100 ps shock wave when $D = 40$ nm, $u_p = 0.7$ km/s); (c) 20 nm (after 40 ps shock wave when $D = 40$ nm, $u_p = 1.1$ km/s); (d) 37.7 nm (after 70 ps shock wave when $D = 40$ nm, $u_p = 1.1$ km/s) and (e) 21.2 nm (after 86 ps shock wave when $D = 30$ nm, $u_p = 0.9$ km/s), respectively.